10 *Inorg. Chem.* **2011**, *50*, 10–12
DOI: 10.1021/ic102133z

Inorganic Chemistry
Communication

New Oxides Showing an Intense Blue Color Based on Mn^{3+} in Trigonal-Bipyramidal Coordination

Hiroshi Mizoguchi, Arthur W. Sleight, and M. A. Subramanian*

Department of Chemistry, Oregon State University, Corvallis, Oregon 97331-4003, United States

Received October 22, 2010

Substitution of Mn^{3+} into the trigonal-bipyramidal sites of oxides with $YbFe_2O_4$-related structures produces an intense blue color because of an allowed d−d transition. This has been demonstrated utilizing a variety of hosts including $ScAlMgO_4$, $ScGaMgO_4$, $LuGaMgO_4$, $ScGaZnO_4$, $LuGaZnO_4$, and $LuGaO_3(ZnO)_2$. The hue of the blue color can be controlled by the choice of the host.

Recently, we have shown that intense, bright-blue colors occur in most of the $YIn_{1-x}Mn_xO_3$ solid-state solutions.[1] This is the first report on the synthesis of oxides with the blue chromophore based on a trigonal-bipyramidal (TBP)-coordinated Mn^{3+} ion. In $YInO_3$, indium takes TBP coordination with pseudo-D_{3h} symmetry (actually C_s symmetry). The Mn^{3+} ions substituted into the indium site show an intense blue color because of an allowed d−d transition. There are relatively few examples of oxides where transition-metal cations occupy TBP sites in oxides, and the $YbFe_2O_4$-type structure is one of the rare examples.[2−8] Figure 1a shows the crystal structure of $YbFe_2O_4$. This may be described as a close packing of O ions with Yb cations in octahedral sites and Fe cations in TBP coordination. The Yb site is often occupied by In, Sc, Y, or smaller rare-earth ions. Both Yb and Fe ions are located on the C_3 axis. The FeO_5 polyhedra share edges with each other and form a $Fe_2O_{2.5}$ layer. The TBP polyhedron is distorted because of Coulomic repulsion between Fe ions, resulting in the formation of FeO_{3+1+1} or FeO_{1+3+1} polyhedra with C_{3v} symmetry.

Kimizuka and co-workers have reported the synthesis and structural analysis for the $(YbFeO_3)(ZnO)_m$ homologous series, as well as $YbFe_2O_4$-type oxides.[9−12] In these structures, the Fe ion has the full D_{3h} symmetry of an ideal TBP when m is even. When m is odd, the $Fe_2O_{2.5}$ layer, which is also observed in the $YbFe_2O_4$ structure, is sandwiched by ZnO layers (wurzite layers). For even m, a $FeO_{1.5}$ layer containing ideal FeO_5 polyhedra is sandwiched by ZnO layers (Figure 1b).

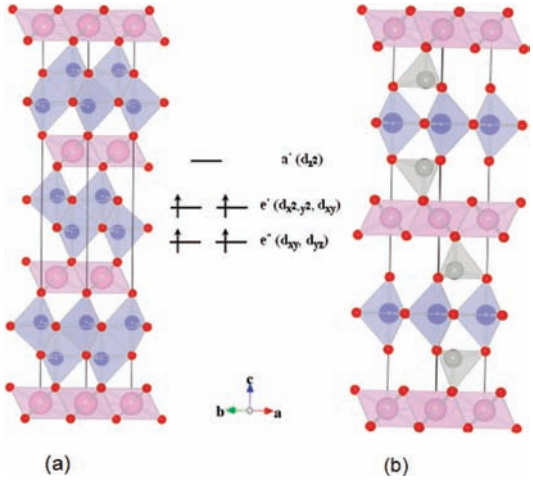

Figure 1. Crystal structures of (a) $YbFe_2O_4$ and (b) $LuFeO_3(ZnO)_2$ showing FeO_5 trigonal bipyramids in blue (Fe, blue spheres; O, red spheres; Yb/Lu, pink spheres; Zn, gray spheres). Schematic energy levels for Mn^{3+} 3d orbitals in TBP coordination are also shown.

Recently, possible applications for $YbFe_2O_4$-type oxides have been suggested. For example, much attention has been given to the magnetodielectric properties of $LuFe_2O_4$ because of strong electrical and magnetic coupling.[13,14] In addition, the transparent conductive properties of $InGaZnO_4$ have

*To whom correspondence should be addressed. E-mail: mas.subramanian@oregonstate.edu.

(1) Smith, A. E.; Mizoguchi, H.; Delaney, K.; Spaldin, N. A.; Sleight, A. W.; Subramanian, M. A. *J. Am. Chem. Soc.* **2009**, *131*, 17084.
(2) Kato, K.; Kawada, I.; Kimizuka, N.; Katsura, T. *Z. Kristallogr.* **1975**, *141*, 314.
(3) Malaman, P. B.; Evrard, O.; Tannieres-Aubry, N.; Courtois, A.; Protas, J. *Acta Crystallogr., Sect. B* **1975**, *31*, 1310.
(4) Kimizuka, N.; Takayama, E. *J. Solid State Chem.* **1982**, *41*, 166.
(5) Nespolo, M.; Isobe, M.; Iida, J.; Kimizuka, N. *Acta Crystallogr., Sect. B* **2000**, *56*, 805.
(6) Kimizuka, M.; Mohri, T. *J. Solid State Chem.* **1985**, *60*, 382.
(7) Barbier, J. J. *Solid State Chem.* **1989**, *82*, 115.
(8) Cava, R. J.; Ramirez, A. P.; Huang, Q.; Krajewski, J. J. *J. Solid State Chem.* **1998**, *140*, 337.
(9) Kimizuka, N.; Mohri, T. J. *Solid State Chem.* **1989**, *78*, 98.
(10) Isobe, M.; Kimizuka, N.; Nakamura, M.; Mohri, T. *Acta Crystallogr., Sect. C* **1994**, *50*, 332.
(11) Kimizuka, N.; Isobe, M.; Nakamura, M. *J. Solid State Chem.* **1995**, *116*, 170.
(12) Keller, I.; Assenmacher, W.; Schnakenburg, G.; Mader, W. *Z. Anorg. Allg. Chem.* **2009**, *635*, 2065.
(13) Ikeda, N.; Ohsumi, H.; Ohwada, K.; Ishii, K.; Inami, T.; Kakurai, K.; Murakami, Y.; Yoshii, K.; Mori, S.; Horibe, Y.; Kito, H. *Nature* **2005**, *436*, 1136.
(14) Subramanian, M. A.; He, T.; Chen, J. Z.; Rogado, N. S.; Calvarese, T. G.; Sleight, A. W. *Adv. Mater.* **2006**, *18*, 1737.

 Published on Web 12/07/2010

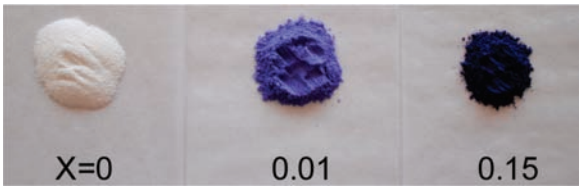

Figure 2. Colors of the powders of $LuGa_{1-x}Mn_xMgO_4$.

been investigated for possible use in transparent transistors.[15,16] The objective of this study was to determine if intense blue oxides could be formed by introducing Mn^{3+} into TBP coordination in other structures.

Samples were prepared from high-purity reactants using high-temperature solid-state reactions, and details are given in the Supporting Information. Details on the data collection of powder X-ray diffraction (XRD), magnetization, and diffuse-reflectance spectra are also included in the Supporting Information. Structure refinements were performed with the Rietveld method, as implemented in the *TOPAS* software package.[17]

All of the samples described in this paper are electrical insulators. All of the samples without Mn substitution are white, except for pale-yellow $LuGaMgO_4$. Mn substitution causes a blue color for $ScGaZnO_4$, $LuGaZnO_4$, and $LuGaO_3(ZnO)_2$ or a bluish-purple color for $ScAlMgO_4$, $ScGaMgO_4$, and $LuGaMgO_4$. Figure 2 shows the colors of some $LuGa_{1-x}Mn_xMgO_4$ samples.

Powder XRD patterns confirmed that $ScAlMgO_4$, $ScGaMgO_4$, $ScGaZnO_4$, $LuGaMgO_4$, and $LuGaZnO_4$ have the $YbFe_2O_4$-type structure and that $LuGaO_3(ZnO)_2$ is isostructural with $LuFeO_3(ZnO)_2$. The XRD pattern of the $ScAlMgO_4$ powder shows weak impurity peaks originating from MgO and $MgAl_2O_4$ (spinel). MgO was dissolved by washing with nitric acid. The formation of residual MgO and $MgAl_2O_4$ indicates a Sc-rich composition for the $ScAlMgO_4$ product. Superlattice peaks due to ordering of Mg/Al on TBP sites were not detected. Structure refinements were based on the space group $R\bar{3}m$. The analysis included the very weak peaks originating from $MgAl_2O_4$. An R of 16% was obtained for the $Sc(Al_{0.5}Mg_{0.5})_2O_4$ model, where Al and Mg are distributed at random on the TBP sites. Next, a split site model for the octahedral site was applied using the 6c site, as used for $LuCuGaO_4$.[8] However, significant improvement of the R value was not obtained. Next, thermal displacement parameters of the cations were fixed at appropriate values, and occupancy factors for the cations were refined. An occupancy of 1.09 was obtained for the TBP site, indicating that the heavier cation is present in the TBP site, as reported for $In(In_{0.2}Ga_{0.8}Mg)O_4$.[7] This conclusion is consistent with the results of our synthesis as mentioned above. Therefore, we considered the model where some Al^{3+} is replaced by Sc^{3+}. A slight improvement of the R value (15.5%) was obtained for the final composition, $Sc(Sc_{0.11}Al_{0.39}Mg_{0.5})_2O_4$. The refinement results are summarized in Table S1 in the Supporting Information. The observed, calculated, and difference patterns are also shown in the Supporting Information (Figure S1). Selected bond distances and angles are listed in Table S2 in the Supporting Information. The M−O distances are 1.89 Å × 3, 1.90 Å, and 2.20 Å, resulting in MO_{4+1} coordination. As the A ion becomes large relative to the M ion, a MO_{1+3+1} coordination appears because of the geometrical constraint. Very recently, single-crystal structural analysis for $ScAlMgO_4$ has been reported by Zhou et al.[18] Although they did not consider the possibility of mixing of the Sc ion into the M site, our results basically agree with their refinements.

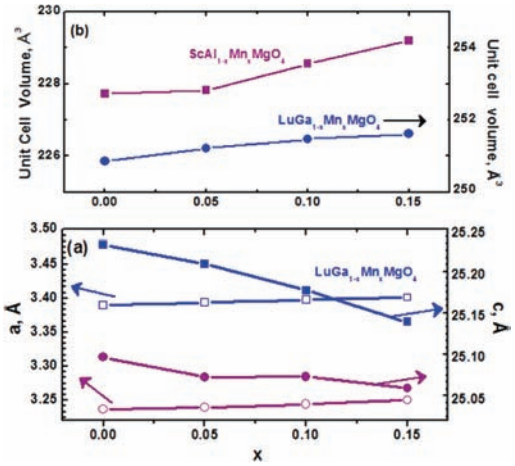

Figure 3. Unit cell edge (a) and volume (b) for $LuGa_{1-x}Mn_xMgO_4$ (blue symbols) and $ScAl_{1-x}Mn_xMgO_4$ (purple symbols).

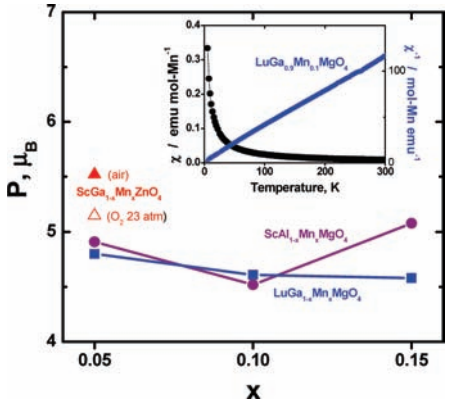

Figure 4. Effective Bohr magneton of the Mn ion for $LuGa_{1-x}Mn_xMgO_4$, $ScAl_{1-x}Mn_xMgO_4$, and $ScGa_{1-x}Mn_xZnO_4$. The inset shows the temperature dependence of χ and χ^{-1} for $LuGa_{0.9}Mn_{0.1}MgO_4$. The direct-current magnetization measurement was done at $H = 500$ Oe. The open and filled red triangles are data for $ScGa_{1-x}Mn_xZnO_4$ samples synthesized under high oxygen pressure and in air, respectively.

Diffraction peaks due to impurity phases were not observed up to $x = 0.15$ for $ScAl_{1-x}Mn_xMgO_4$ and $LuGa_{1-x}Mn_xMgO_4$. Figure 3 shows the unit cell volume and unit cell edges for these oxides. According to Shannon,[19] the sizes of Mn^{3+} and Mn^{2+} are larger than that of Ga^{3+} or Mg^{2+}. Therefore, the results shown in Figure 3 confirm the formation of a solid-state solution with Mn. The decrease in the a cell edge with increasing x is expected because of the empty d_{z^2} orbital of Mn^{3+}. Similarly, the formation of a solid-state solution up to 5% was confirmed in $ScGa_{1-x}Mn_xZnO_4$ and $LuGa_{1-x}Mn_xO_3(ZnO)_2$.

(15) Orita, M.; Takeuchi, M.; Sakai, H.; Tanji, H. *Jpn. J. Appl. Phys.* **1995**, *34*, L1550.
(16) Nomura, K.; Ohta, H.; Ueda, K.; Kamiya, T.; Hirano, M.; Hosono, H. *Science* **2003**, *300*, 1269.
(17) Cheary, R. W.; Coelho, A. A. *J. Appl. Crystallogr.* **1992**, *25*, 109.
(18) Zhou, H.; Liang, Y.; Huang, W.; Ye, N.; Zou, Y. *Chin. J. Struct. Chem.* **2009**, *28*, 947.
(19) Shannon, R. D. *Acta Crystallogr., Sect. A* **1976**, *32*, 751.

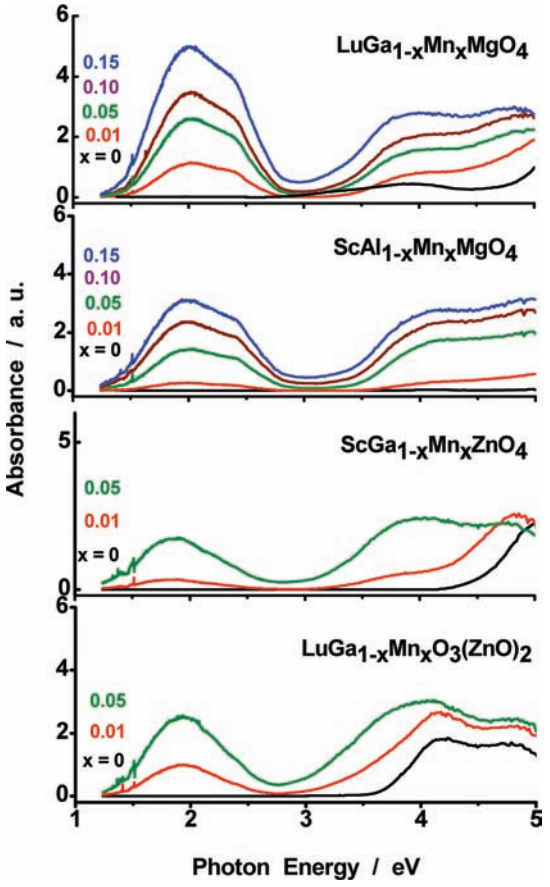

Figure 5. Diffuse-reflectance spectra for $LuGa_{1-x}Mn_xMgO_4$, $ScAl_{1-x}Mn_xMgO_4$, $ScGa_{1-x}Mn_xZnO_4$, and $LuGa_{1-x}Mn_xO_3(ZnO)_2$.

Many $YbFe_2O_4$-type oxides containing Mn^{2+} have been reported.[4,5] They were synthesized by solid-state reactions under low oxygen pressures to maintain Mn^{2+}. There have been no reports about these oxides containing Mn^{3+}. To confirm the presence of Mn^{3+}, magnetic susceptibility measurements were conducted. The inset in Figure 4 shows the temperature dependence of χ and inverse χ per Mn for $LuGa_{0.9}Mn_{0.1}MgO_4$. The susceptibility increases in the low-temperature region, indicating spin alignment. This curve obeys the Curie−Weiss law, $\chi = C/(T - \theta)$, in the measured temperature region. The effective Bohr magneton, μ_{eff}, calculated from the Curie constant obtained by the fitting to the Curie−Weiss law is plotted in Figure 4. The theoretical effective Bohr magneton, μ_{eff}, was calculated from the equation $\mu_{eff} = 2[S(S + 1)]^{1/2}$ to be 5.92, 4.90, and 3.87 for $S = {}^5/_2$ (d^5), ${}^4/_2$ (d^4), and ${}^3/_2$ (d^3), respectively. Therefore, the experimental μ_{eff} values for $ScAl_{1-x}Mn_xMgO_4$ and $LuGa_{1-x}Mn_xMgO_4$ are close to 4.90, indicating Mn^{3+} $3d^4$ (high spin) in these oxides.

As shown in Figure 4, the Mn valence in $ScGa_{1-x}Mn_xZnO_4$ depends on the partial oxygen pressure of the synthesis conditions. The use of an oxygen pressure of 23 atm (at 700 °C) during the synthesis oxidizes Mn to the trivalent state. On the other hand, the formation of Mn^{3+} in $AB_{1-x}Mn_xMgO_4$ occurs even under air. This seems to be an inductive effect, whereby the highly electropositive Mg ion in the $ABMgO_4$ lattices lowers the energy of the O 2p states, thereby stabilizing the higher oxidation state of Mn.

Figure 5 shows the optical absorption spectra for Mn-substituted oxides. Band gaps in the undoped phases are evident only when Zn is present. The band gaps for $ScGaZnO_4$ and $LuGaO_3(ZnO)_2$ are estimated to be 4.5 and 3.7 eV, respectively. The former agrees well with that determined by Blasse et al. from photoluminescence excitation spectra.[20] As Mn^{3+} is introduced, two new absorption bands appear for all of the samples. One of these bands is located at ~2 eV and is the origin of the bluish color. The other appears at about ~4 eV. Figure S2 in the Supporting Information shows the change of the intensity of the former peak for $ScAl_{1-x}Mn_xMgO_4$ and $LuGa_{1-x}Mn_xMgO_4$. As x increases, the intensity tends to saturate. However, these results clearly indicate that the newly formed absorption band at 2 eV originates from the TBP-coordinated Mn^{3+} ion. The small splitting of the absorption band at about 2 eV in these phases as well as in the $YIn_{1-x}Mn_xO_3$ phases can be attributed to the fact that the symmetry of the TPB site does not possess the full D_{3h} symmetry of an ideal TBP.

The blue-colored $ScGa_{1-x}Mn_xZnO_4$ and $LuGa_{1-x}Mn_xO_3(ZnO)_2$ samples have a single absorption band at 1.9 eV. This is ascribed to an allowed transition from e′ to a_1 in D_{3h} symmetry, the ideal symmetry for TBP coordination. A transition from e″ to a_1 is forbidden. The a_1 antibonding state originates from the Mn $3d_{z^2}$−O_{ap} 2p interaction; thus, the position of the absorption band near 2 eV depends on the Mn−O_{ap} distances. All samples show a charge transfer from O 2p to a_1 in the region 3.5−4.0 eV. As x increases, this absorption band rapidly broadens.

We have shown that the blue or bluish-purple color occurs in Mn^{3+}-substituted $YbFe_2O_4$-related oxides, which have TBP coordination. Control of the ligand field of Mn^{3+} changes the color from blue to bluish-purple. This study confirms that intense blue pigments can be designed by introducing Mn^{3+} into various structures containing TBP coordination and is not limited to hexagonal AMO_3 phases.

Acknowledgment. This work was supported by NSF Grant DMR 0804167. We thank Dr. Janet Tate for optical measurements and Dr. F. Funabiki for molecular orbital calculations.

Supporting Information Available: Experimental details (synthesis and characterization) and structure information tables and data (powder XRD, optical, and magnetic). This material is available free of charge via the Internet at http://pubs.acs.org.

(20) Blasse, G.; Dirksen, G. L.; Kimizuka, N.; Mohri, T. *Mater. Res. Bull.* **1986**, *21*, 1057.